

## Metamorphic P-T evolution and fluid inclusion study of Bodonch, Zereg, Sharga and Altai areas, Southwestern Mongolia

ZORIGTKHUU, Oyun-Erdene<sup>1\*</sup>, TSUNOGAE, Toshiaki<sup>1</sup>, Batulzii Dash<sup>2</sup>

<sup>1</sup>University of Tsukuba, <sup>2</sup>Mongolian University of Science and Technology

The Altai Orogen in the southwestern margin of the Central Asian Orogenic Belt (one of the largest accretionary and collisional orogen in the world) extends from Russia and East Kazakhstan to the west, through Northern China, to southwestern Mongolia to the east. It contains various volcano-sedimentary rocks that were deformed and metamorphosed under various pressure-temperature (P-T) conditions from greenschist to amphibolite and partly granulite facies. We report first detailed petrological and fluid inclusion data of pelitic schists and mafic rocks from Bodonch, Zereg, Sharga, and Altai areas, southwestern Mongolia, which occupy a significant part of the Paleozoic history of the Altai Orogen in the southwestern margin of the Central Asian Orogenic Belt (or Altaids), and discuss P-T evolution of the area.

Zereg, Sharga, and Altai areas contains mafic to ultramafic rocks and pelitic schists with various mineral assemblages such as amphibole + plagioclase + muscovite + chlorite + calcite, serpentine + olivine + chromium spinel + iron oxide, serpentine + olivine + clinopyroxene + talc, chlorite + muscovite + plagioclase + quartz + ilmenite. In the context of traditional terrain tectonics (Badarch et al., 2002) the belt belongs to the Hovd and Dariv terrains and classified as accretionary wedge and metamorphic belt with uncertain tectonic affinity.

Bodonch area contains pelitic schists and amphibolites with various mineral assemblages such as garnet + kyanite + staurolite + biotite + plagioclase, garnet + biotite + staurolite + cordierite, and amphibole + quartz + plagioclase + garnet + ilmenite.

We performed detailed petrologic, geothermobarometric and mineral equilibrium modelling studies on the rocks from Bodonch area and obtained peak P-T condition of 640-690<sup>0</sup>C /6.3-10.7 kbar and clockwise path from the area. The peak high-pressure amphibolite-facies condition and clockwise P-T evolution of the area estimated for the first time in this study is consistent with available reports of other localities in the Altai Orogen outside Mongolia. Three categories of fluid inclusions have been observed in quartz: dominant primary and secondary inclusions, and least dominant pseudosecondary inclusions. As quartz in the samples are texturally associated with biotite, kyanite, and staurolite, which were probably formed during peak metamorphism, we regard that the primary fluid inclusions trapped in the quartz grains probably preserve peak metamorphic fluids. The melting temperatures of all the categories of inclusions lie in the narrow range of -57.5 to -56.6<sup>0</sup>C, close to the triple point of pure CO<sub>2</sub>. Homogenization of fluids occurs into liquid phase at temperature range between -33.3 to +19.4<sup>0</sup>C, which convert into densities in the range of 0.78 to 1.09 g/cm<sup>3</sup>. The results of this study, together with the primary and pseudosecondary nature of the inclusions, indicate CO<sub>2</sub> was the dominant fluid component during the peak amphibolite-facies metamorphism of the study area. Therefore, this is a rare example of CO<sub>2</sub> -rich fluid inclusions trapped in amphibolite-facies rocks.

Keywords: fluid inclusion, mineral equilibrium modeling, Altai Orogeny, Central Asian Orogenic Belt, Mongolia

## Fluid and cooling-driven reaction exsolution in garnet porphyroblasts: near-peak history of UHT granulites, EGB, India

DAS, Kaushik<sup>1\*</sup>, TOMIOKA, Naotaka<sup>2</sup>, BOSE, SANKAR<sup>3</sup>, ANDO, Jun-ichi<sup>1</sup>

<sup>1</sup>Department of Earth and Planetary Sciences, Hiroshima University, <sup>2</sup>ISEI, Okayama University, Misasa, <sup>3</sup>Department of Geology, Presidency University, Kolkata, India

Intergrowth textures in porphyroblastic assemblages of granulites are extremely important to decipher the near-peak evolutionary history of deep continental crust undergoing several pulses of orogenic cycles. Eastern Ghats granulite belt of India evolved through Proterozoic orogenic events has occurrences of aluminous granulites and associated quartzofeldspathic gneisses where garnet porphyroblasts contain nanometer- to micrometer-thick ilmenite needles oriented crystallographically. Such garnet porphyroblasts are presumably a product of dehydration melting reaction(s) of Ti-rich phlogopite during the pre-peak metamorphic stage leading to the UHT peak condition. The high oxygen fugacity condition during this stage promoted the enrichment of possible Ti-bearing andradite component in garnet porphyroblasts in appropriate bulk chemistry. In the subsequent post-peak cooling-dominated history with lowered oxygen fugacity, Ti-bearing components of garnet porphyroblasts decomposed to rhombohedral oxide solid solution (ilmenite-hematite). Transmission electron microscopic study of the garnet porphyroblasts and needle-shaped monomineralic ilmenite solid solution indicates that though there is an overall parallelism of [011]\* of host garnet and [011]\* of ilmenite, structural coherence between the two phases is progressively lost during growth from thin to thick needles. We argue that cooling from high-temperature peak metamorphic condition promoted growth of ilmenite solid solution through reaction-exsolution process within garnet porphyroblasts. Integrated temperature and fO<sub>2</sub> information during deep crustal evolution can thus be retrieved from the detailed petrographic, SEM, EPMA and TEM studies of high-grade granulites.

Keywords: Oriented ilmenite needles, Garnet porphyroblasts, UHT granulites, Reaction-exsolution, EGB, India

## Interpretation for geochemical diversity of the Neogene granitoid plutons in the Izu Collision Zone

SAITO, Satoshi<sup>1\*</sup>

<sup>1</sup>Research Institute for Humanity and Nature

Neogene granitoid plutons are widely exposed in the Izu Collision Zone in central Japan, where the northern tip of the Izu-Bonin arc (juvenile oceanic arc) has been colliding with the Honshu arc (mature island arc) since middle Miocene. Three main granitoid plutons are distributed in this area: Tanzawa Plutonic Complex (TPC), Kofu Granitic Complex (KGC), and Kaikomagatake pluton (KP). The TPC and southern part of the KGC were intruded in submarine volcanic piles of the Izu-Bonin arc, while the KP and the northern and central parts of the KGC were intruded in Shimanto metasedimentary rocks of the Honshu arc. In this study, I compile geochemical data of these three plutons (Kawate and Arima 1998; Saito et al. 2004; Saito et al. 2007a,b; Saito et al. in press), and propose a petrogenetic model explaining the geochemical diversity of granitoid plutons in the Izu Collision Zone.

The TPC consists of tonalite and trondhjemite and characterized by low K<sub>2</sub>O contents (< 2.5 wt %), whereas the KP is characterized by relatively high K<sub>2</sub>O contents (3-5 wt %) and composed of granodiorite and monzogranite. The rocks of KGC range from tonalite, trondhjemite, granodiorite to granite, and show wide variation of K<sub>2</sub>O contents (0.5-7 wt %). Previous petrogenetic studies on the plutons have been suggested that (1) the TPC formed by lower crustal anatexis of juvenile basaltic rocks occurring in the Izu-Bonin arc (Kawate and Arima 1998), (2) the KGC formed by anatexis of hybrid lower crustal sources comprising of both basaltic rocks of the Izu-Bonin arc and metasedimentary rocks of the Honshu arc (Saito et al. 2007b), and (3) the KP formed by anatexis of hybrid lower crust consisting of K-rich rear-arc crust of the Izu-Bonin arc and metasedimentary rocks of the Honshu arc (Saito et al. in press). These studies collectively suggest that the chemical diversity within the Izu Collision Zone granitoid plutons reflects the chemical variation of basaltic sources (i.e., across-arc chemical variation in the Izu-Bonin arc) as well as variable contribution of the metasedimentary component in the source region.

### References:

Kawate S, Arima M (1998) Tanzawa plutonic complex, central Japan: Exposed felsic middle crust of Izu-Bonin-Mariana arc. *Island Arc* 7:342-358.

Saito S, Arima M, Nakajima T, Kimura J-I (2004) Petrogenesis of Ashigawa and Tonogi granitic intrusions, southern part of the Miocene Kofu Granitic Complex, central Japan: M-type granite in the Izu arc collision zone. *J Mineral Petrol Sci* 99:104-117.

Saito S, Arima M, Nakajima T (2007a) Hybridization of a shallow 'I-type' granitoid pluton and its host migmatite by magma-chamber wall collapse: the Tokuwa pluton, central Japan. *J Petrol* 48:79-111.

Saito S, Arima M, Nakajima T, Misawa K, Kimura J-I (2007b) Formation of distinct granitic magma batches by partial melting of hybrid lower crust in the Izu arc collision zone, central Japan. *J Petrol* 48:1761-1791.

Saito S, Arima M, Nakajima T, Tani K, Miyazaki T, Senda R, Chang Q, Takahashi T, Hirahara Y, Kimura J-I (in press, published online on Sep 2011) Petrogenesis of the Kaikomagatake granitoid pluton in the Izu Collision Zone, central Japan: implications for transformation of juvenile oceanic arc into mature continental crust. *Contrib Mineral and Petrol*, DOI 10.1007/s00410-011-0689-1.

Keywords: Izu Collision Zone, Granite, Kofu Granitic Complex, Tanzawa Plutonic Complex, Kaikomagatake pluton

## Spatial variations in Hf isotopic compositions of Quaternary volcanic rocks in North-eastern Japan Arc

HIRAHARA, Yuka<sup>1\*</sup>, TAKAHASHI, Toshiro<sup>1</sup>, MIYAZAKI, Takashi<sup>1</sup>, CHANG, Qing<sup>1</sup>, SENDA, Ryoko<sup>1</sup>, YOSHIDA, Takeyoshi<sup>2</sup>, BAN, Masao<sup>3</sup>, KURITANI, Takeshi<sup>4</sup>, FUJINAWA, Akihiko<sup>5</sup>, OHBA, Tsukasa<sup>6</sup>, HAYASHI, Shintaro<sup>6</sup>, KIMURA, Jun-Ichi<sup>1</sup>

<sup>1</sup>JAMSTEC, <sup>2</sup>Tohoku Univ., <sup>3</sup>Yamagata Univ., <sup>4</sup>Oosaka-city Univ., <sup>5</sup>Ibaragi Univ., <sup>6</sup>Akita Univ.

The dual Quaternary volcanic chains of the North-eastern Japan (NEJ) Arc sit 100 km and 150-170 km above the top of the subducting Pacific Plate. We focus on a particular variation in the isotopic compositions of Quaternary volcanic rocks in the NEJ Arc because isotope data are useful for estimating the influence of subducting components on mantle wedges. In general, slab-derived materials from subducting plates add to mantle wedges, and these materials induce the generation of island arc magma.

In this study, we report a new spatial variation of Hf isotopic compositions in combination with Sr-Nd-Pb isotopes and trace element compositions. Although a high-field-strength elements (HFSE), Hf is one of them, rare earth elements (REE), and large-ion lithophile element (LILE) behave as incompatible elements during mantle-melting processes, they distinctively separate from each other into preferentially partitioned aqueous fluids due to the increased solubility from LILE, REE to HFSE. Therefore, Hf isotopes in combination with other geochemical signatures serve as identification of metasomatic agents in subduction-related magma generation.

On the rear arc (RA) side, we collected samples from the Chokai, Sannome-gata, Moriyoshi, and Kampu volcanoes. On the volcanic front (VF) side, we collected samples from the north area (the Iwate and Akita-koma-ga-take volcanoes), the central area (the Zao and Azuma volcanoes), and the south area (the Nasu and Takahara volcanoes).

The RA volcanic rocks have limited and slightly enriched Sr-Nd-Pb isotopic ratios and trace element compositions as compared to those of mid-ocean ridge basalts (MORB) from the Japan Sea. In contrast, the compositions of the VF samples tend to be more enriched with wide variations. The Sr-Nd-Hf isotopes in the VF rocks tend to be more enriched as one goes from north to south, and the sample with the most enriched isotopic compositions is from the Takahara volcano. In the correlation diagrams of the Sr-Nd isotopic compositions, the trend from the RA to the VF samples appears as a mix of depleted MORB mantle (DMM) and enriched oceanic sediments or continental crust materials. However, the variation in the Hf-Nd isotopes in the VF samples could not be explained by a model of bulk-mixing between DMM and subducted oceanic sediments. Moreover, these isotopic ratios decrease with increasing SiO<sub>2</sub> content. These observations indicate that the variations in the VF samples were formed during processes of magmatic evolution, such as assimilation-fractional crystallization (AFC) or mixing with silicic magma, thus resulting in enriched isotopic compositions. Furthermore, the VF rocks have different Pb isotopic compositions in different area, which indicates that such a varied trend was probably caused by a variety of contaminated crust compositions. In contrast, the Sr-Nd-Hf-Pb isotopic ratios for the RA rocks suggest that their enriched isotopic compositions as compared to MORBs were most likely influenced by the enriched subducting components, and not the crustal material, because the values of the isotopic ratios become constant when their SiO<sub>2</sub> content increases.

Keywords: NE Japan arc, Quaternary volcanic rocks, Spatial variations in isotopic compositions, Hf isotopes

## Origin of "black olivines"

HOSHIKAWA, Chihiro<sup>1\*</sup>, MIURA, Makoto<sup>1</sup>, ARAI, Shoji<sup>1</sup>

<sup>1</sup>Earth Sci., Kanazawa Univ.

Rocks of SDW (spinel-rich dunite-wehrlite) suite of the Horoman peridotite complex are characterized by fresh black-colored olivines. The black color is caused by numerous minute inclusions in olivine. The inclusions are homogeneously distributed in olivine grains of the SDW. They are different from the secondary inclusions of magnetite associated with hydrous minerals aligned in olivine both in the SDW dunite and in the MHL harzburgite. The inclusions are abundant in dunites from the central part of the SDW layer, whereas they are scarcely observed in olivines near the contact with the MHL harzburgite. The MHL harzburgite do not contain olivines with such inclusions.

Raman spectroscopy revealed that the numerous minute inclusions consist of magnetite and orthopyroxene. It is very difficult to form such magnetite inclusions by secondary oxidation of olivines. They are possibly subsolidus exsolution products from OH-bearing olivines, precipitated from a hydrous magma. The "black olivine" in dunite can be an indicator for involvement of hydrous melt. Fresh olivines with black colors are frequently found in course-grained dunites.

## High-NiO olivine in the dunite enveloping the concordant chromitite from the Wadi Hilti, northern Oman ophiolite

MIURA, Makoto<sup>1\*</sup>, ARAI, Shoji<sup>1</sup>

<sup>1</sup>Department of Earth Sciences, Kanazawa University

Two types of podiform chromitite, concordant and discordant, are exposed on the same cliff in the mantle section of Wadi Hilti, northern Oman ophiolite. Chromian spinel grains only from the concordant chromitite contain thin lamellae of diopside and enstatite. This indicates that the concordant chromitite has experienced cooling, and probably decompression, for a longer prolonged period than the discordant one. Olivines in the dunite enveloping the concordant chromitite is sometimes extraordinarily high in NiO (up to >0.5wt%), suggesting subsolidus Ni diffusion from the chromitite. This is not the case for the dunite envelope around the discordant chromitite. Ni has moved over about 10cm from the boundary between the concordant chromitite and dunite, which is consistent with the appearance of pyroxenes lamellae in spinel of the concordant chromitite. According to the well-known Ni diffusion coefficient in olivine, the high-NiO olivine in the dunite envelope can constrain the cooling duration of the concordant chromitite. Podiform chromitites are enigmatic in origin, and their origins should be systematically classified to understand concerning mantle processes. Their temporal relationship is a clue to solve this problem.

Keywords: Olivine, Ni diffusion, Podiform chromitite, Oman ophiolite

## High temperature oxidation of lherzolite xenolith from Oku district, Oki-Dogo Island, Japan: evidence in olivine

EJIMA, Terumi<sup>1\*</sup>, AKASAKA, Masahide<sup>1</sup>, Hiroaki OHFUJI<sup>2</sup>

<sup>1</sup>Department of Geoscience, Graduate School of Science and Engineering, Shimane University, Matsue 690, <sup>2</sup>Geodynamics Research Center, Ehime University, Matsuyama 790-8577, Japan

Ejima et al. (2011) reported Fe<sup>3+</sup> from olivine in lherzolite xenolith from Oku-district, Oki-Dogo Island, Shimane Prefecture, and pointed out two possibilities of generation of Fe<sup>3+</sup> in olivine: 1) Olivine was incorporated Fe<sup>3+</sup> at upper mantle condition; 2) Fe<sup>3+</sup> was generated in olivine by high temperature oxidation in host basalt magma. In order to solve this problem, we investigated a brown zone (about 0.3 mm) distributed at the rim of olivine in the margin of the xenolith in touch with host basalt, using methods of electron probe microanalysis (EMPA), high resolution transmission electron microscopy (HRTEM) and Raman spectroscopy.

The brown zone consisted of forsterite with Fo<sub>69</sub> (mol%), which is Fe-rich than that at the core part (Fo<sub>81</sub>) of the xenoliths. No impurity was detected by EMPA, although the Fe-O vibration peaks of hematite and magnetite were detected by Raman spectroscopic analysis. HRTEM observation revealed existence of dislocation cores parallel to (001) of olivine structure, and electron diffraction spots of olivine consisting of the brown zone showed weak streak along the c-axis. However no precipitate such as hematite or magnetite was detected by HRTEM observation. Thus, the Fe-O vibrations observed in Raman spectra can be attributed to very short-range hematite and magnetite structure clusters in olivine, but not to hematite and magnetite phases.

On the basis of the results of the present study, genetic process of hematite and magnetite structure clusters at the rim of olivine in the margin of the Oku lherzolite xenolith in touch with host basalt is considered as follows: 1) a part of Fe<sup>2+</sup> on the rim of olivine was changed to Fe<sup>3+</sup> by high temperature oxidation, and vacant octahedral sites were generated; 2) Fe<sup>3+</sup> in olivine increased with high temperature oxidation, and hematite and magnetite structure clusters were formed in olivine structure; 3) in the region of hematite structure clusters, vacant layers (dislocation cores) parallel to (001) of olivine structure were formed. Therefore, crystallization of hematite and magnetite along the dislocation cores by further high temperature oxidation is expected.

Previous studies by annealing experiments of olivine in air reported crystallization of laihunite. However, in the olivine of the Oku lherzolite xenolith, laihunite was not detected, and existence of hematite and magnetite structures clusters in olivine are considered instead. Thus, two ways of crystallization of precipitates by high temperature oxidation can be proposed: 1) crystallization of laihunite -> hematite -> magnetite with increasing temperature; 2) crystallization of magnetite -> hematite with decreasing temperature, where the crystallization of laihunite is quite difficult. The latter case corresponds to olivine in the Oku lherzolite xenolith.

We conclude that Fe<sup>3+</sup> within olivine from the Oku lherzolite xenolith (Ejima et al., 2011) was generated by high temperature oxidation underwent during the transportation from the upper mantle to the surface.

Keywords: olivine, lherzolite xenolith, oxidation state of Fe, high temperature oxidation

## A technique for EBSD analyses of phyllosilicates in petrographic sections and determination of polytypes in lepidolite

INOUE, Sayako<sup>1\*</sup>, KOGURE, Toshihiro<sup>1</sup>

<sup>1</sup>Earth & Planetary Sci., Univ. Tokyo

Applications of Electron backscatter diffraction (EBSD) to obtain crystallographic information of minerals in petrographic thin sections are increasing in mineralogy and petrology. However, platy phyllosilicates that mostly appear with their silicate layers terminated by the surface of the thin section generally do not show sharp EBSD patterns in spite of gentle mechanical polishing using colloidal silica. Transmission electron microscopy (TEM) examination indicated that this is due to crystal bending of phyllosilicates from the surface to a few micrometers in depth, caused by the polishing process (Fig. a). Ion beam etching commonly used to prepare TEM specimens was found to be applicable to remove the surface region with crystal bending (Fig. b and c). As a result, clear and sharp EBSD patterns were acquired from the phyllosilicates (micas, chlorite, etc.) in petrographic thin sections, by which their crystal orientations and polytypes were unambiguously determined. This technique was applied to the determination of polytypes of lepidolite, a lithium-rich aluminous mica whose general composition is expressed as  $K(Li, Al)_{2-3}(Si, Al)_4O_{10}(OH, F)_2$ .

The mica structure generates six standard polytypes expressed as  $1M$ ,  $2M_1$ ,  $2M_2$ ,  $2O$ ,  $3T$  and  $6R$ . They are divided into two subfamilies: *subfamilies* A and B.  $1M$ ,  $2M_1$  and  $3T$  are classified into *subfamilies* A, and  $2M_2$ ,  $2O$  and  $6R$  are classified into *subfamilies* B (Backhaus and Durovic 1984). Using EBSD pattern, it is possible to distinguish the two *subfamilies* (Kogure 2002). We investigated lepidolite from a lithium pegmatite in Myoken-san, Ibaraki, where various polytypes have been reported (Kogure and Bunno 2004). EBSD analyses of lepidolite crystals in petrographic thin sections showed that polytypes with different subfamilies coexist within a single crystal: The outside was  $1M$  (*subfamilies* A) and inside was  $2M_2$  (*subfamilies* B).

### References

Backhaus, K. O. and Durovic, S. (1984) Polytypism of micas. I. MDO polytypes and their derivation. *Clays and Clay Minerals*, 32, 453-463.

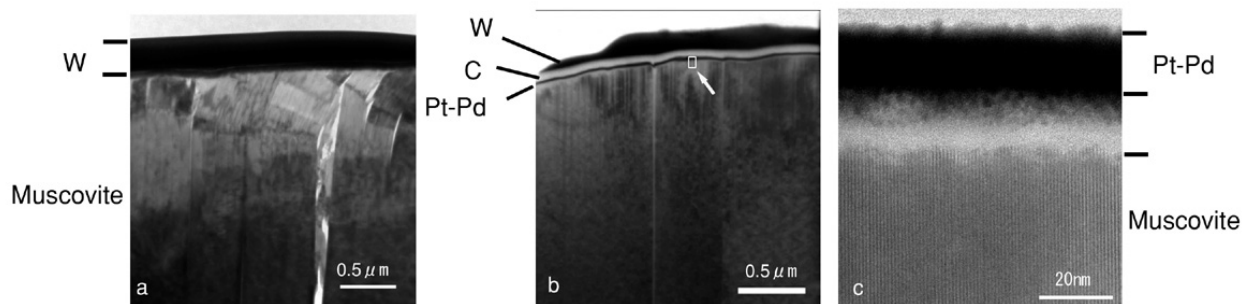
Kogure, T. (2002) Identification of polytypic groups in hydrous phyllosilicates using Electron Back-Scattering Patterns (EBSPs), *American Mineralogist*, 87, 1678-1685.

Kogure, T. and Bunno, M. (2004) Investigation of polytypes in lepidolite using electron back-scattered diffraction. *American Mineralogist*, 89, 1680-1684.

### Figure

(a) TEM image of muscovite near the polished surface with colloidal silica. Tungsten (W) was coated for surface protection in the FIB process. (b) TEM image of muscovite near the surface etched by ion milling. Pt-Pd and carbon film were coated after ion milling to identify the specimen surface. (c) High-resolution TEM image of the area marked with square in b.

Keywords: EBSD, phyllosilicates, ion milling, petrographic thin section, polytype, lepidolite





## Distribution of cations at two tetrahedral sites in $\text{Ca}_2\text{MgSi}_2\text{O}_7$ - $\text{Ca}_2\text{Fe}^{3+}\text{AlSiO}_7$ series synthetic melilite and its relation

HAMADA, Maki<sup>1\*</sup>, AKASAKA, Masahide<sup>1</sup>

<sup>1</sup>Shimane Univ.

Synthetic melilites,  $\text{W}_2\text{T}_1\text{T}_2\text{O}_7$ , were analyzed to determine the distribution of  $\text{Fe}^{3+}$  between two different tetrahedral sites (T1 and T2), and the relationship between ionic substitution and incommensurate structure in melilite. Melilites on the join  $\text{Ca}_2\text{MgSi}_2\text{O}_7$  (kermanite: Ak)- $\text{Ca}_2\text{Fe}^{3+}\text{AlSiO}_7$  (ferrialuminium gehlenite: FAGeh) system were synthesized from starting materials with compositions of  $\text{Ak}_{100}$  (100Ak),  $\text{Ak}_{80}\text{FAGeh}_{20}$  (80Ak),  $\text{Ak}_{70}\text{FAGeh}_{30}$  (70Ak) and  $\text{Ak}_{50}\text{FAGeh}_{50}$  (by sintering at 1200-1250 °C and 1 atm. The synthetic melilites were analyzed using X-ray powder diffraction, <sup>57</sup>Fe Mossbauer, and high-resolution transmission electron microscopic methods. The average chemical compositions and end-member components, Ak, FAGeh and Geh ( $\text{Ca}_2\text{Al}_2\text{SiO}_7$ ), of the synthetic melilites were  $\text{Ca}_{2.015}\text{Mg}_{1.023}\text{Si}_{1.981}\text{O}_7$  (100Ak),  $\text{Ca}_{2.017}\text{Mg}_{0.788}\text{Fe}^{3+}_{0.187}\text{Al}_{0.221}\text{Si}_{1.791}\text{O}_7$  (80Ak),  $\text{Ca}_{1.995}\text{Mg}_{0.695}\text{Fe}^{3+}_{0.258}\text{Al}_{0.318}\text{Si}_{1.723}\text{O}_7$  (70Ak) and  $\text{Ca}_{1.982}\text{Mg}_{0.495}\text{Fe}^{3+}_{0.449}\text{Al}_{0.519}\text{Si}_{1.535}\text{O}_7$  (50Ak), respectively.

The site populations at the T1 and T2 sites were  $[0.788\text{Mg}+0.054\text{Fe}^{3+}+0.158\text{Al}]\text{T}_1[0.056\text{Fe}^{3+}+0.153\text{Al}+1.791\text{Si}]\text{T}_2$  for 80Ak,  $[0.695\text{Mg}+0.105\text{Fe}^{3+}+0.200\text{Al}]\text{T}_1[0.112\text{Fe}^{3+}+0.165\text{Al}+1.723\text{Si}]\text{T}_2$  for 70Ak and  $[0.495\text{Mg}+0.173\text{Fe}^{3+}+0.332\text{Al}]\text{T}_1[0.281\text{Fe}^{3+}+0.153\text{Al}+1.535\text{Si}]\text{T}_2$  for 50Ak (apfu: atoms per formula unit), respectively. The results indicate that  $\text{Fe}^{3+}$  is distributed at both the T1 and the T2 sites. The mean T1-O distance decreases with the substitution of  $\text{Fe}^{3+} + \text{Al}^{3+}$  for  $\text{Mg}^{2+}$  at the T1 site, whereas the mean T2-O distance increases with substitution of  $\text{Fe}^{3+} + \text{Al}^{3+}$  for  $\text{Si}^{4+}$  at the T2 site, causing decrease in the *a* dimension and increase of the *c* dimension.

The existence of incommensurate structure in all synthetic melilites at room temperature was confirmed by Mossbauer and  $\text{CuK}_{\alpha 1}$  X-ray line profile analyses. The Mossbauer spectra of the melilites consist of two doublets assigned to  $\text{Fe}^{3+}$  at the T1 site and two or three doublets to  $\text{Fe}^{3+}$  at the T2 site, which imply the existence of multiple T1 and T2 sites with different site distortions, respectively. The existence of two T1 sites is not influenced by ionic substitution. Conversely, the splitting of T2 sites becomes more remarkable with the substitution of  $\text{Fe}^{3+} + \text{Al}^{3+}$  for  $\text{Si}^{4+}$  which results in the increase of volume and site distortion of the  $\text{T}_2\text{O}_4$ -tetrahedra.

Incommensurate structure in melilite has been interpreted rather statically, based on the crystal structure of kermanite, that the incommensurate structure is caused by the misfit between the tetrahedral sheet and the polyhedral sheet. However, as found in this study, effect of ionic substitution at the T1 and T2 sites on the formation of incommensurate structure is also significant. The first factor is the site distortion arising from the distribution of cations with different ionic radii in the T1 and T2 sites. Even though the cation sites are symmetrically equivalent in the average structure, each tetrahedron which is occupied by different cation(s) has variant volume. The second factor is the site distortions caused by the difference of adjacent coordination polyhedra around tetrahedra. Therefore, in Ak-FAGeh melilite solid solutions, the site distortions caused by the ionic substitution at the tetrahedral sites play important role on the formation of the incommensurate structure.

Keywords: synthetic melilite, incommensurate structure, X-ray powder diffraction method, Electron diffraction, Mossbauer spectroscopy

## Study on classification of terrestrial impact structures and concentration of impact-related carbon light elements

MIURA, Yasunori<sup>1\*</sup>

<sup>1</sup>Visiting (Univs.)

Terrestrial impact structures indicating remnants of the surface activity are classified largely as follows:

1) Type 1 impact structure: Impact crater structures formed at crystalline igneous and sedimentary rocks on large continental crust are almost this type remained at present continents. Eject direction from target rocks is opposite direction for ejecta with vapor.

2) Type 2 impact structure: Impact structures formed at sedimentary and limestone basement rocks of sea (ocean) - water is buried and broken by plate-movements, which should be checked precisely by drilled and physical explorations. Soft or porous target rocks of the type II impact produce comparatively penetration of ejecta or light gas vapor in the progress direction.

The type 2 structure is classified to sea-bottom and lands by remained sites of impact remnants. Sea-bottom type 2 structure can be explored due to young formation, but land type 2 remained at lands is classified more at lowlands remained structures (Akiyoshi and Takamatsu), and at highland remained at the summit (Santa Fe, USA etc.).

The Santa Fe impact structure which has been explored by research scientists of the University of New Mexico in 2011 fall during my stay at the UNM University, is to be classified as highland type 2 structure because we found new limestone breccias with impact-related carbon-bearing micro-materials by our FE-ASEM works in this study.

Terrestrial elemental concentration of mineral deposits formed at high temperature, can be formed at impact breccias to produce high contents of carbon and rare-earth elements, as well as previous igneous magmatic melting on the Earth planet.

The present idea of impact concentration can be checked at the Apollo lunar breccias samples with the elemental concentration, which will be applied significantly to other planets and Asteroids for next new exploration of resources and rock-minerals.

Keywords: impact structure, classification, impact carbon-bearing materials, ocean impact, concentration reservoir, limestone breccias